

04
/

SECTION III

MODIFIED BIOTAR AND CATADIOPTRIC SYSTEMS

by



STAT

It was clear at the start of this study that an advance in the state of the art would be necessary to achieve the type of imagery required. A catadioptric system seemed to be the most plausible approach because secondary spectrum is most easily controlled in such systems. However, the advantages of an unsilhouetted aperture led to a preliminary examination of a refractive form.

A lens form invented by Dr. James G. Baker and built by the Perkin-Elmer Corporation as a 24-inch f/3.5 apochromat was chosen as a possible basic form. This lens is essentially a 6-element Biotar with five additional elements mounted between the two halves of the Biotar, as shown in Figure 3. It was hoped that by the use of glasses with improved deviation from the standard partial dispersions, the number of elements required for secondary spectrum correction could be reduced. For this purpose Schott type KzFS-4 was tried in the central group, and Schott type LaF-10 was tried as the glass to be used in the negative elements of the outer groups.

The investigation of this form was continued until it was determined that correcting imagery and secondary spectrum to the extent necessary would require more elements than there were in Baker's original form. Since the elements are rather thick, such a design would be very heavy and much of the advantage of the speed of an f/2 lens would be lost due to the light losses in transmission through the lens. Meeting the requirement of 60% transmission through the lens seemed hopeless with this form.

For the catadioptric system, two additional aims were added to those in the specifications to make the result more useful. These were a flat field, and the positioning of the image plane where it would be easily accessible.

The flat field cameras described by Dr. James G. Baker in Proceedings of The American Philosophical Society, Vol. 82, pp. 339-349(1940) were chosen as a promising starting point. For a description of these optical systems, see also E.H. Linfoot, Recent Advances in Optics, London,

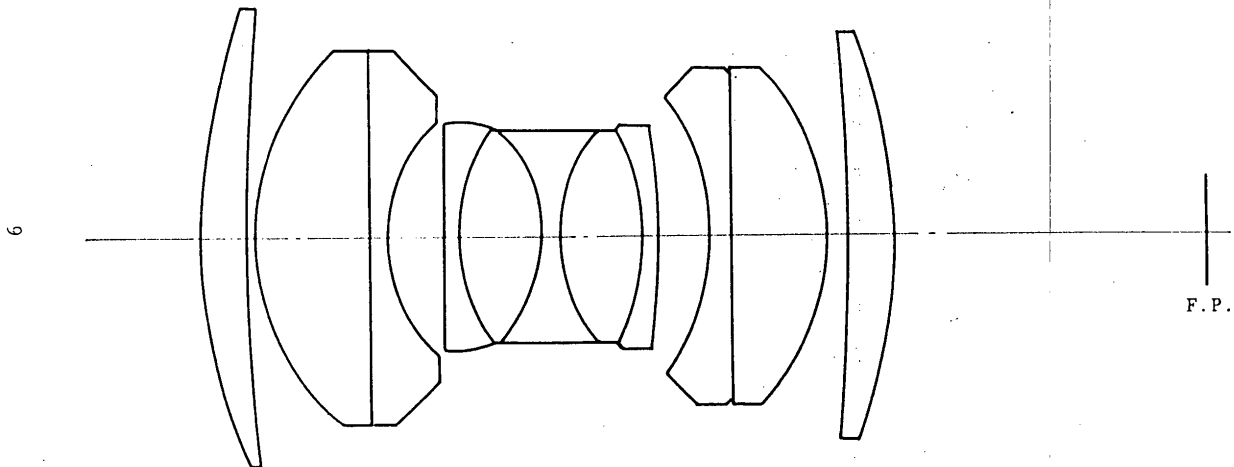


Figure 3. 24" f/3.5 Apochromat, Optical Design

Oxford University Press, 1955, pp. 257-270. These cameras consist of two mirrors arranged in the Cassegrain configuration with an aspheric corrector plate in front of the mirrors.

Of the Baker cameras, the form which he called type B was chosen as the easiest to fabricate. In this system the primary mirror is moderately aspheric and the secondary mirror is spherical.

In the publication mentioned above, Dr. Baker calculated the maximum ray error in a 12-inch $f/2.5$ system at a semi-field angle of 4 degrees as .009 mm. According to the aims of the present contract, 80% of the rays traced for a spot diagram in a 12-inch $f/2.0$ system with a semi-field of 5 degrees are to have a maximum error of .0014 mm. Since all the rays of a spot diagram for an $f/2.5$ system include only 64% of the rays of an $f/2.0$ system of the same focal length, the improvement desired is a factor of the order of 10.

The limiting error in the Baker cameras is one known as oblique spherical aberration, a variation of spherical aberration with field angle. This arises mainly at the corrector plate which is foreshortened for off-axis pencils, making them tend to be over-corrected. To reduce this effect, a concentric shell with its center of curvature at the corrector plate was introduced. Such a shell introduces over-corrected spherical aberration which by symmetry is the same in all parts of the field if the pupil of the system is at its center of curvature. The over-correction required of the corrector plate is thus reduced, thereby reducing the variation of this over-correction with field angle.

The introduction of a concentric shell does not effect any of the other third order aberrations except Petzval sum and longitudinal color.

In accordance with a suggestion made by Dr. Baker, the corrector plate was made achromatic, that is, it was made of two plates of opposite asphericity, one of crown glass and one of flint glass. Under these conditions, the variation of spherical aberration with color is easily controlled. Table III gives the third-order aberrations and color variations of the final system design.

The Petzval sum was restored by departing from the equality of curvatures of the two mirrors. The parameters available for correcting this system are the thickness and location of the concentric shell, the distribution of asphericity between the primary mirror and corrector plates, and the spacing between the elements subject to the condition that the image plane remain accessible.

Extended computations resulted in the system shown in Figure 5. As seen in the spot diagrams, the imagery is better than required by the specifications throughout the 5 degree semi-field for all light in the spectral range e (5461) to C (6563). Table IV gives the

coordinates of the points from which the spot diagrams were plotted. These were obtained by tracing rings through the system. In the spot diagrams the circle represents the first Airy dark band for the wavelength in question.

The size of the secondary mirror (R_g of Figure 4) was chosen so that 25% of the energy of an axial pencil is obscured. Enhanced reflective surfaces on the two mirror surfaces would bring their reflectivity to 98%. Assuming a transmission of 98% at each air-glass surface and allowing for the absorption losses in glass as given on Smithsonian Physical tables, ninth revised edition, 1954, p. 512, Table 526, the transmission of this system was calculated to be 64%. This is somewhat better than the 60% transmission required by the specifications.

Taking the pupil stop in the position shown, the relative transmission at 5 degrees half field was computed as 83%. This again is somewhat better than the 75% called for in the specifications. Figures 9, 13, and 15 show the actual shape of the pupil at each field angle for which spot diagrams are shown.

The length of the system measured from its front surface to the focal plane is 17.05 inches or 1.42 times its focal length. For this system, this is the minimum length for which no baffling is required.

The image plane is flat and accessible. The spot diagrams are taken in an image plane 155.182 mm from the secondary mirror.

The catadioptric system shown in Figure 4 meets all the objectives stated in the specifications. For an accurate description of the performance of the system, an analysis would have to be made taking diffraction into account. However, this catadioptric system will give better imagery than any hitherto known 12-inch f/2.0 anastigmat which covers a 10-degree total field.

TABLE II
CATADIOPTRIC SYSTEM, LENS FORMULA

Surface Number	Radius	Glass Thickness	Air Separation	Glass Type	N_c	N_d	N_e	Clear Aperture
1		5.922		611/588	1.60793	1.61100	1.61357	176.0
2*	+913.9		0.148					174.9
3**	+928.8	7.402		621/362	1.61610	1.62100	1.62520	174.9
4			151.052					174.5
5	-155.74	65.920		517/645	1.51461	1.51700	1.51899	152.7
6	-221.66		158.755					180.0
7***	-342.77		-111.400					207.6
8	-304.13		155.182***					91.62

*ASPHERIC: $x = 5.4712 \times 10^{-4} y^2 + 5.9702 \times 10^{-9} y^4 - 1.9969 \times 10^{-13} y^6 - 1.1367 \times 10^{-17} y^8 - 1.137 \times 10^{-22} y^{10}$

**ASPHERIC: $x = 5.3830 \times 10^{-4} y^2 + 5.9185 \times 10^{-9} y^4 - 1.2377 \times 10^{-13} y^6 - 7.0457 \times 10^{-18} y^8 - 7.047 \times 10^{-13} y^{10}$

***ASPHERIC: $x = -342.77 - (342.77^2 - y^2)^{1/2} - 4.316 \times 10^{-11} y^4 - 8.90 \times 10^{-16} y^6 + 3.2 \times 10^{-25} y^{10}$

***Distance to plane of best imagery (Geometrical).
Stop is 123.5mm from surface No. 4
Diameter of stop is 152.3mm for f/2.0

12

TABLE III						
CATADIOPTRIC SYSTEM						
THIRD-ORDER ABERRATIONS AND CHROMATIC VARIATION						
Surface No.	B dB	F dF	C dC	E dE	a	b
1	.00000 .00000	.00000 .00000	.00000 .00000	-.00124 -.00005	.00000	-.00092
2	.04079 .00039	.00181 .00002	.00118 .00001	.00124 .00000	.00142	.00092
3	-.04109 -.00061	-.00179 -.00003	-.00118 -.00001	-.00125 .00000	-.00226	-.00148
4	.00000 .00000	.00000 .00000	.00000 .00000	.00125 .00000	.00000	.00148
5	.07969 .00024	.00000 .00000	.00000 .00000	.00000 .00000	.00427	.00000
6	-.02471 -.00005	.00000 .00000	.00000 .00000	.00000 .00000	-.00343	.00000
7	-.11096	-.00537	-.00047	.00033	.00000	.00000
8	.05606	.00540	.00052	-.00107	.00000	.00000
Σ	-.00022 -.00003	.00005 -.00001	-.00005 .00000	-.00074 -.00000	.00000	.00000

Note: $y=3.0276S$, $u=0$, $y_p=.01275$, $u_p=.08749$, $u'_g=-.25$, $P=-.00221$,
 $dP=.00006$, $\lambda=.00005$. All dimensions in inches, first line is
3rd.order aberration, second line chromatic variation (e-C).
Positive values denote overcorrected aberrations.

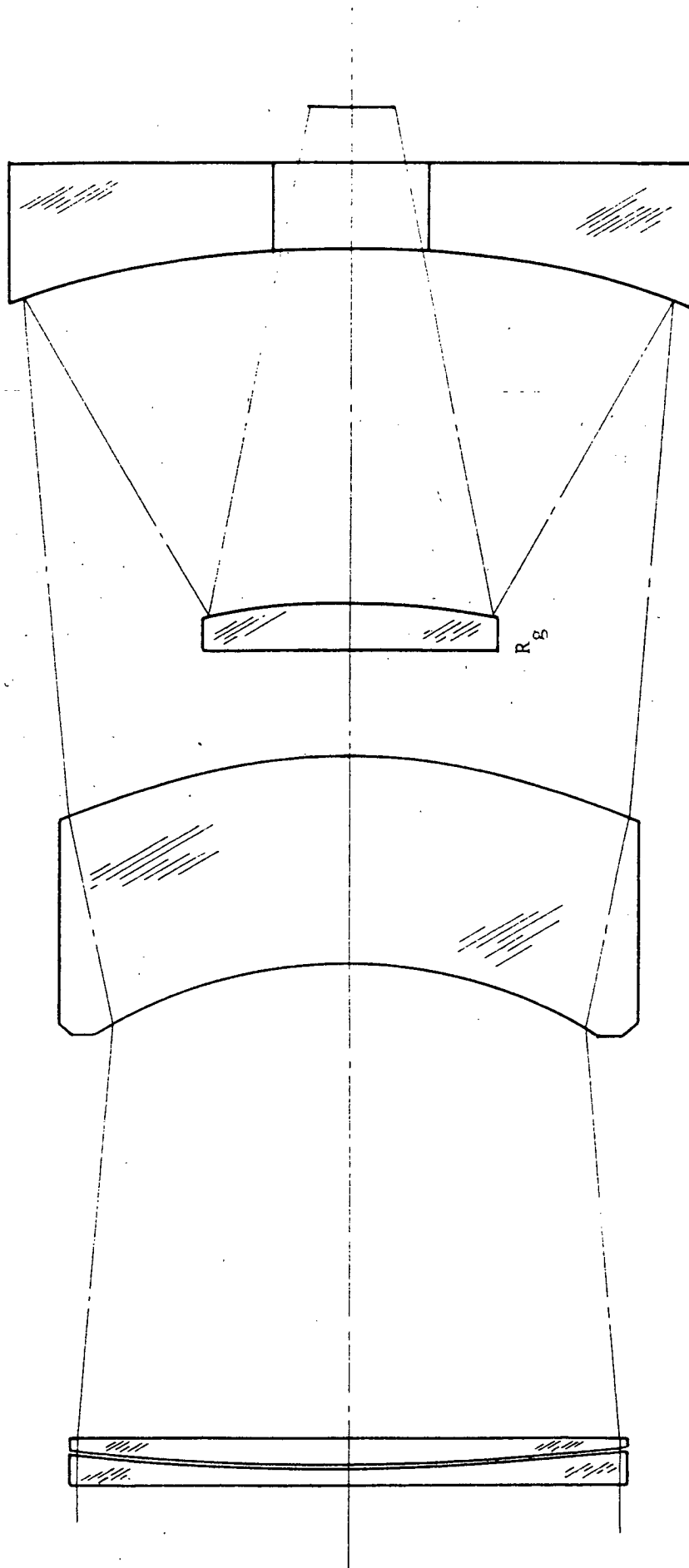


Figure 4. Catadioptric System, Optical Design

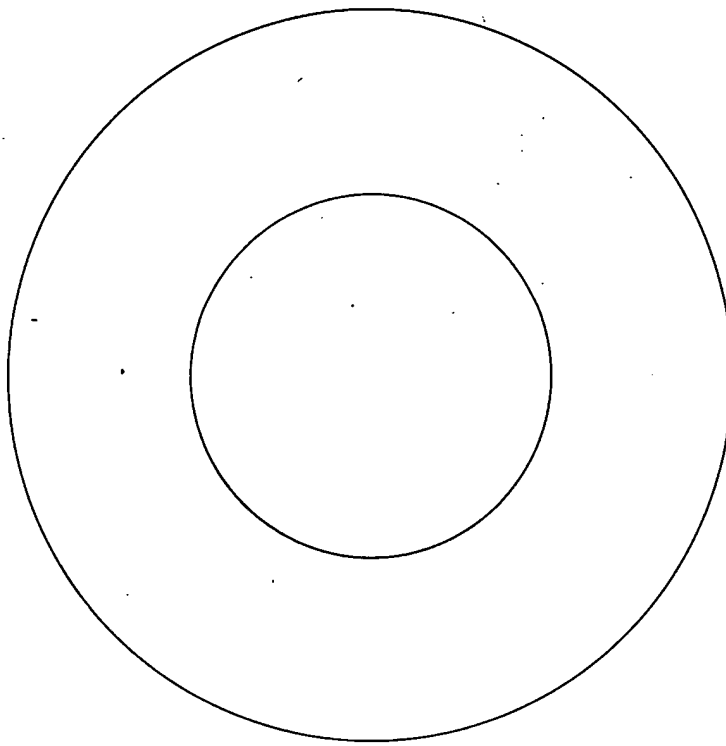


Figure 5. Catadioptric System, Axial Pupil

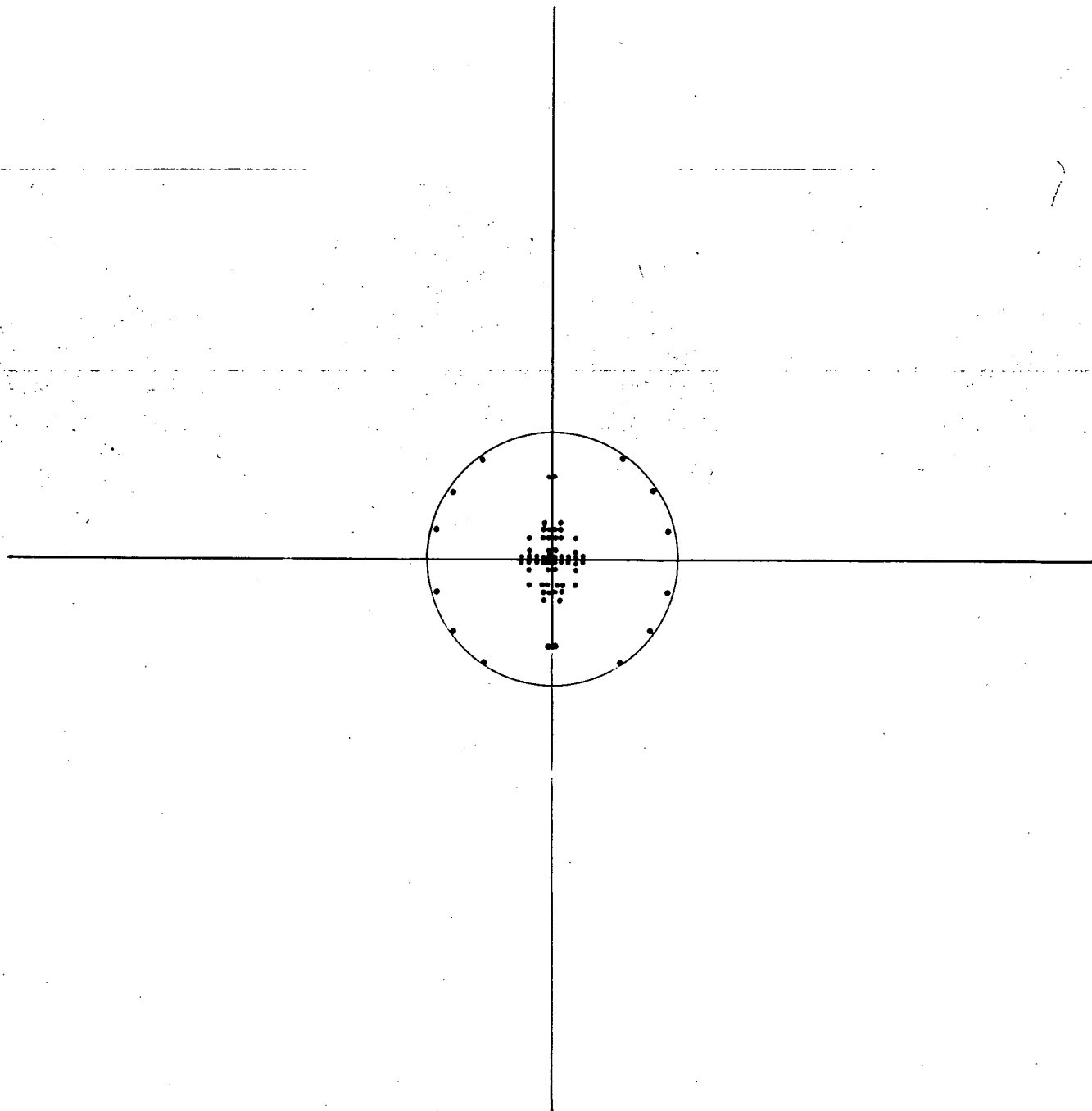


Figure 6. Spot Diagram, Axial Bundle, $\lambda - 6563$ (C-line)

3.0

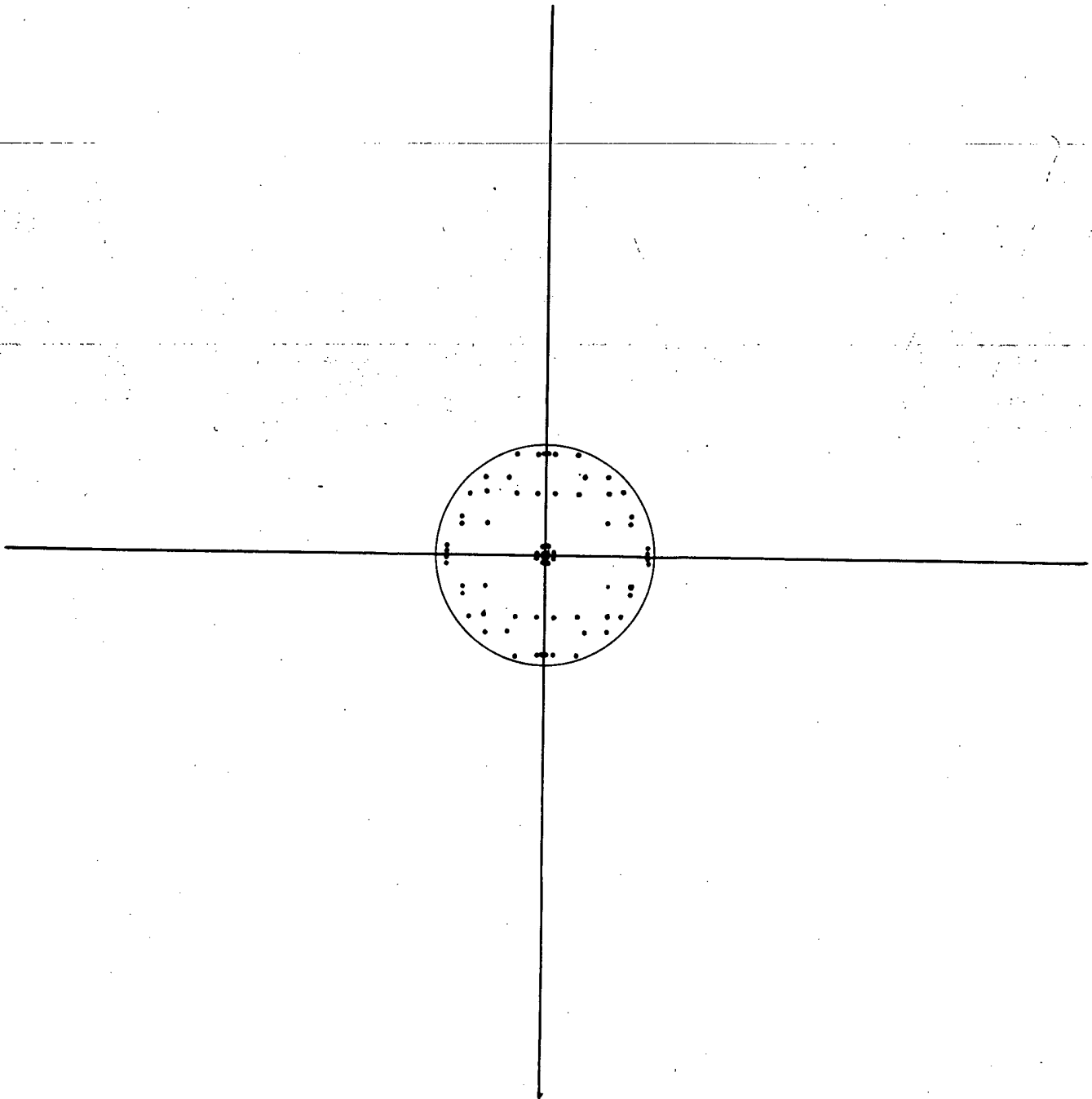


Figure 7. Spot Diagram, Axial Bundle, $\lambda - 5893$ (D-line)

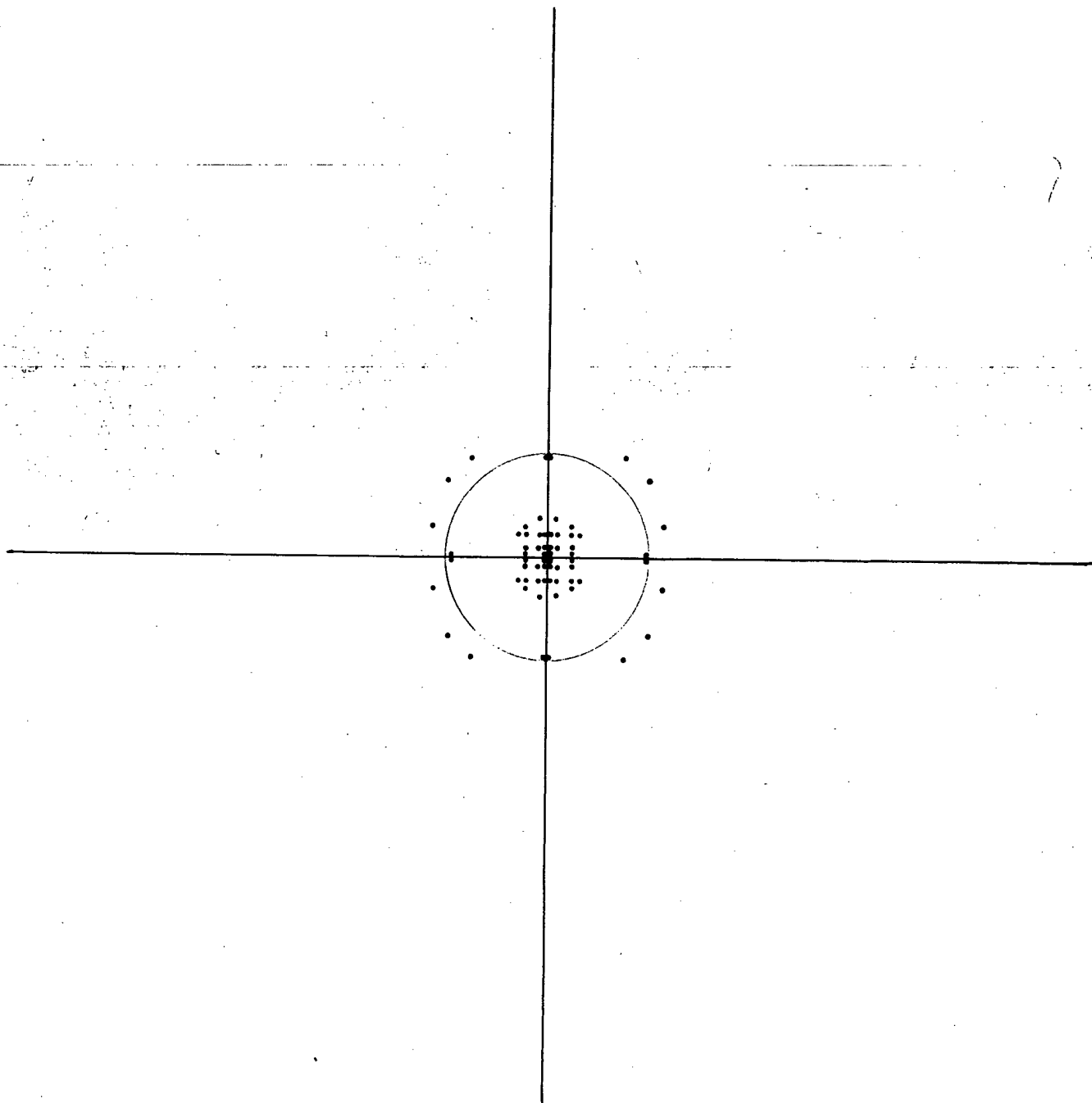


Figure 8. Spot Diagram, Axial Bundle, $\lambda - 5461$ (e-line)

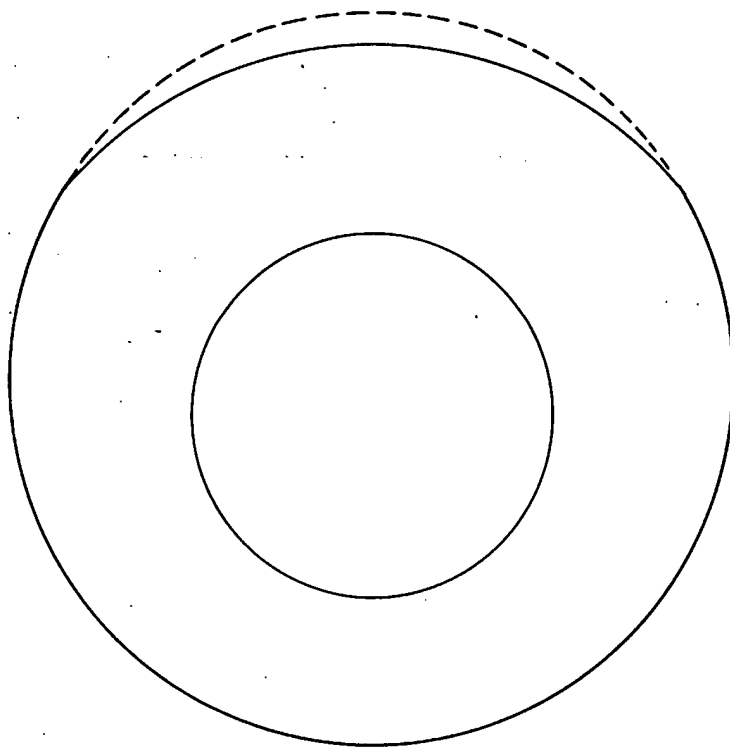


Figure 9. Pupil 3' Off-Axis

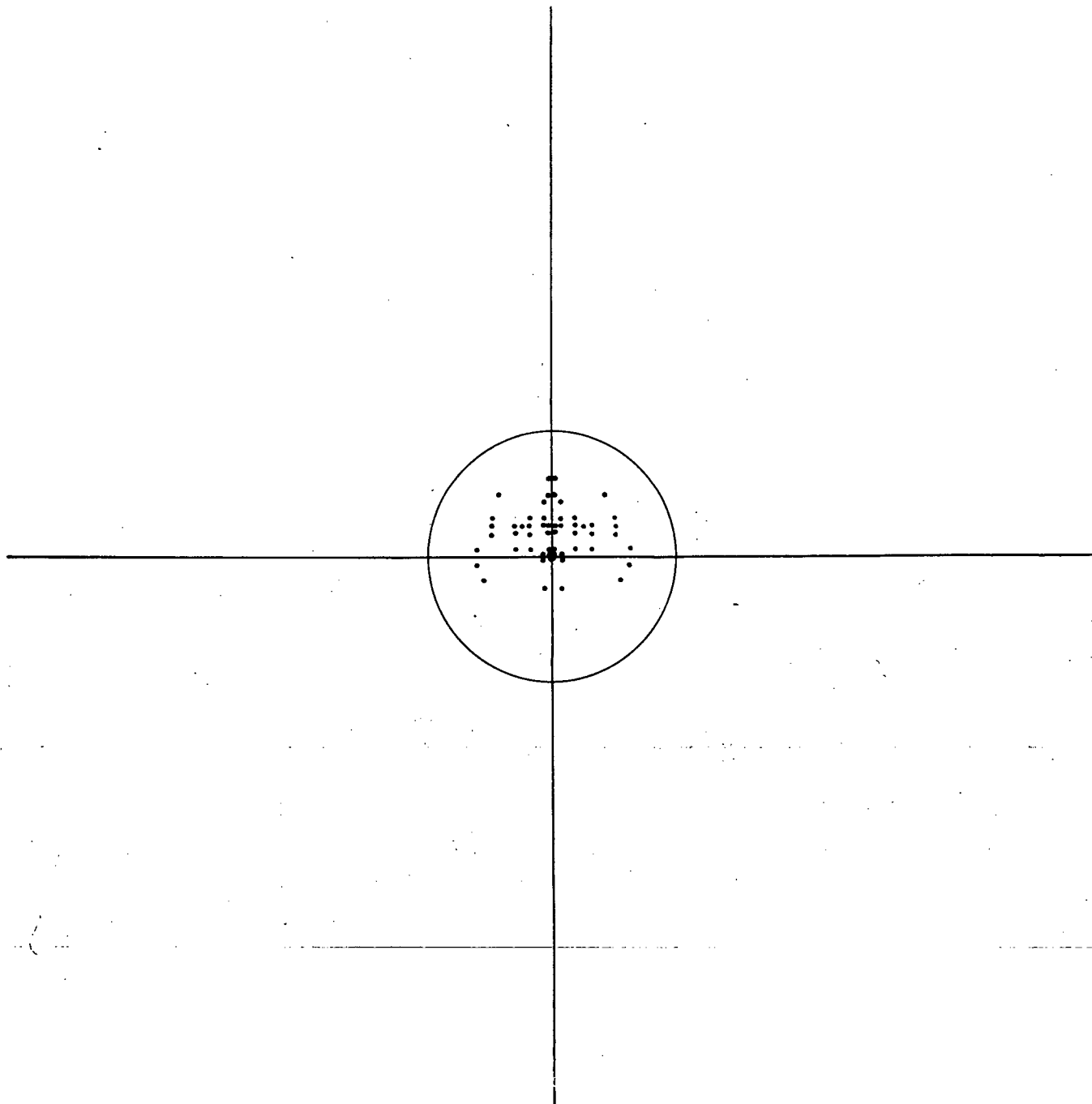


Figure 10. Spot Diagram, 3° Off-Axis $\lambda = 6563$ (C-line)

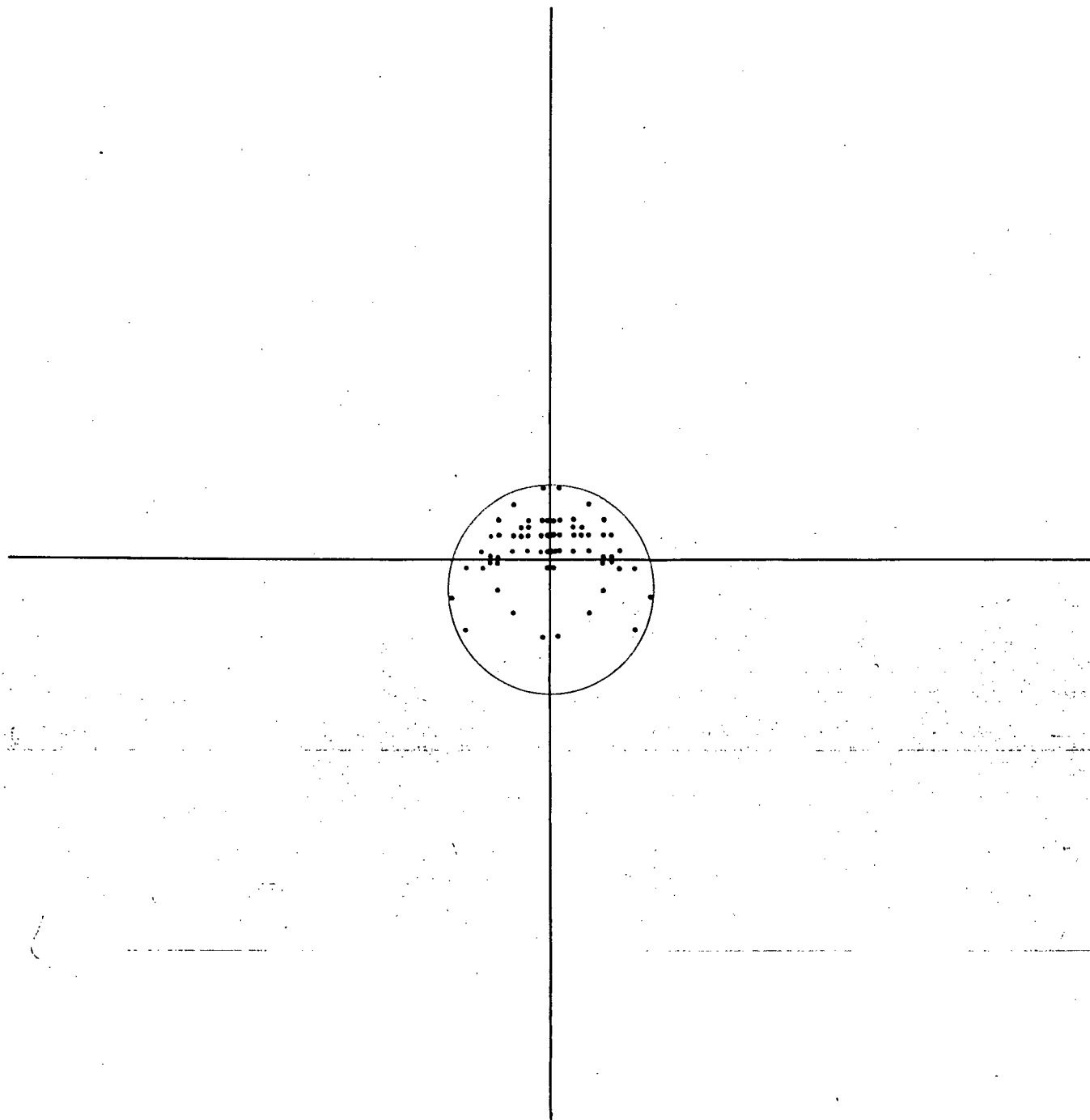


Figure 12. Spot Diagram, 3' Off-Axis $\lambda = 5461$ (e-line)

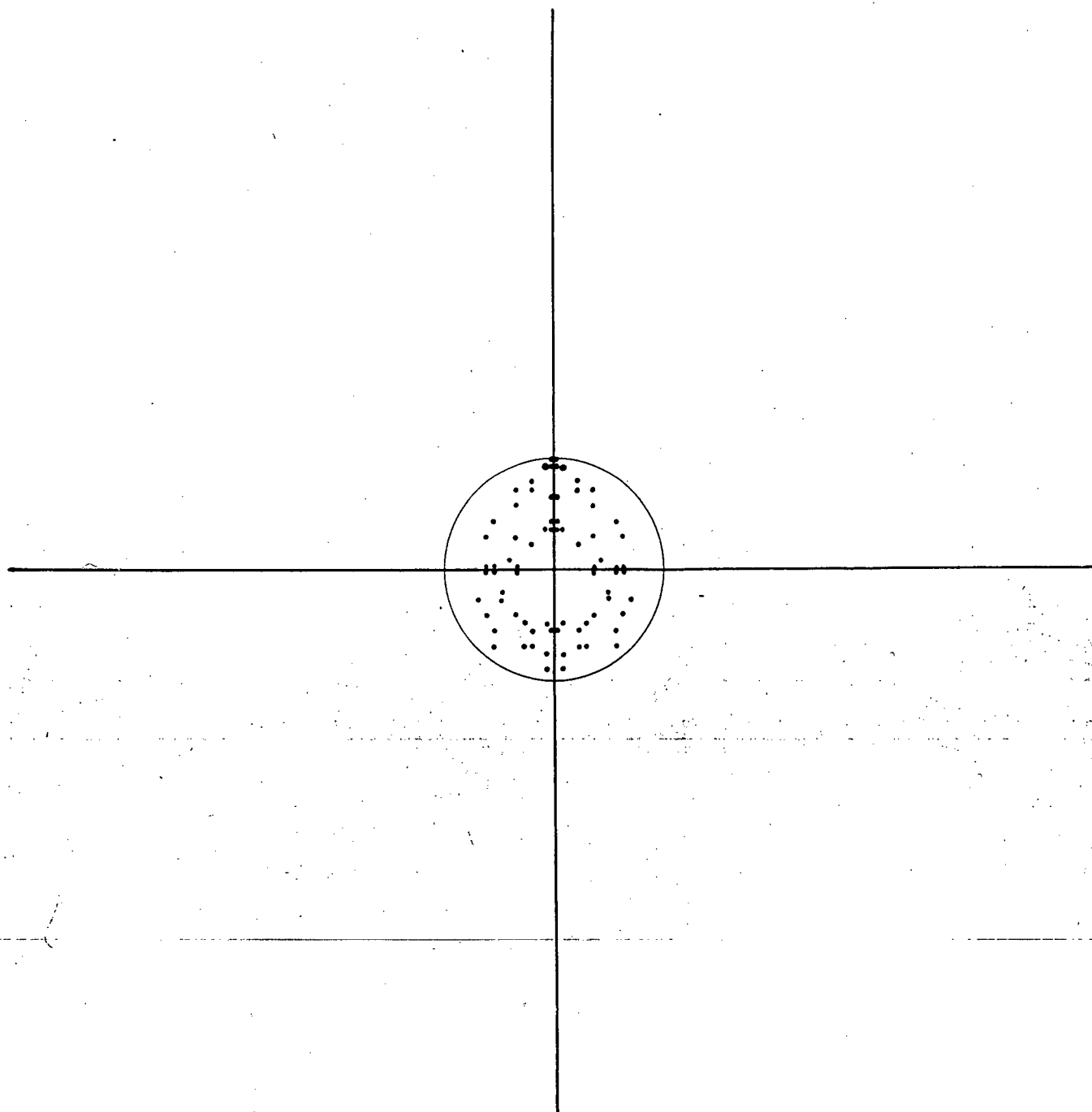


Figure 11. Spot Diagram, 3 Off-Axis $\lambda = 5893$ (D-line)

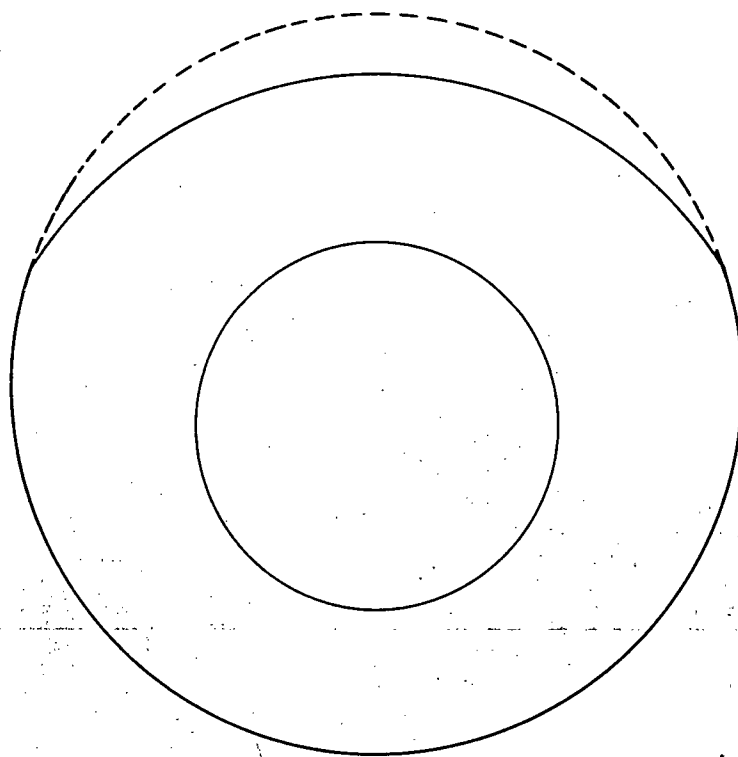


Figure 13. Pupil 4° Off-Axis

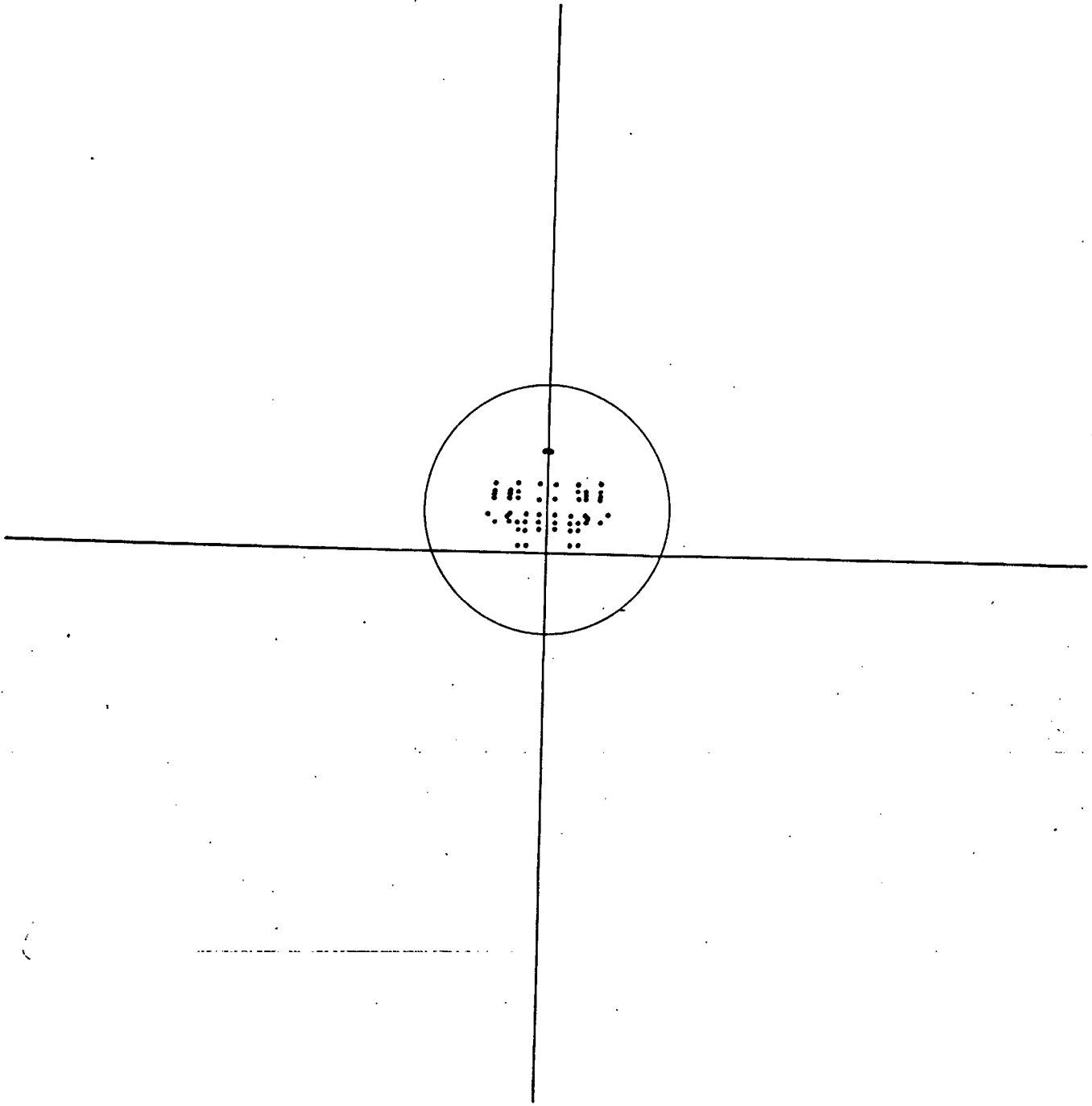


Figure 14. Spot Diagram, 4' Off-Axis $\lambda = 6563$ (C-line)

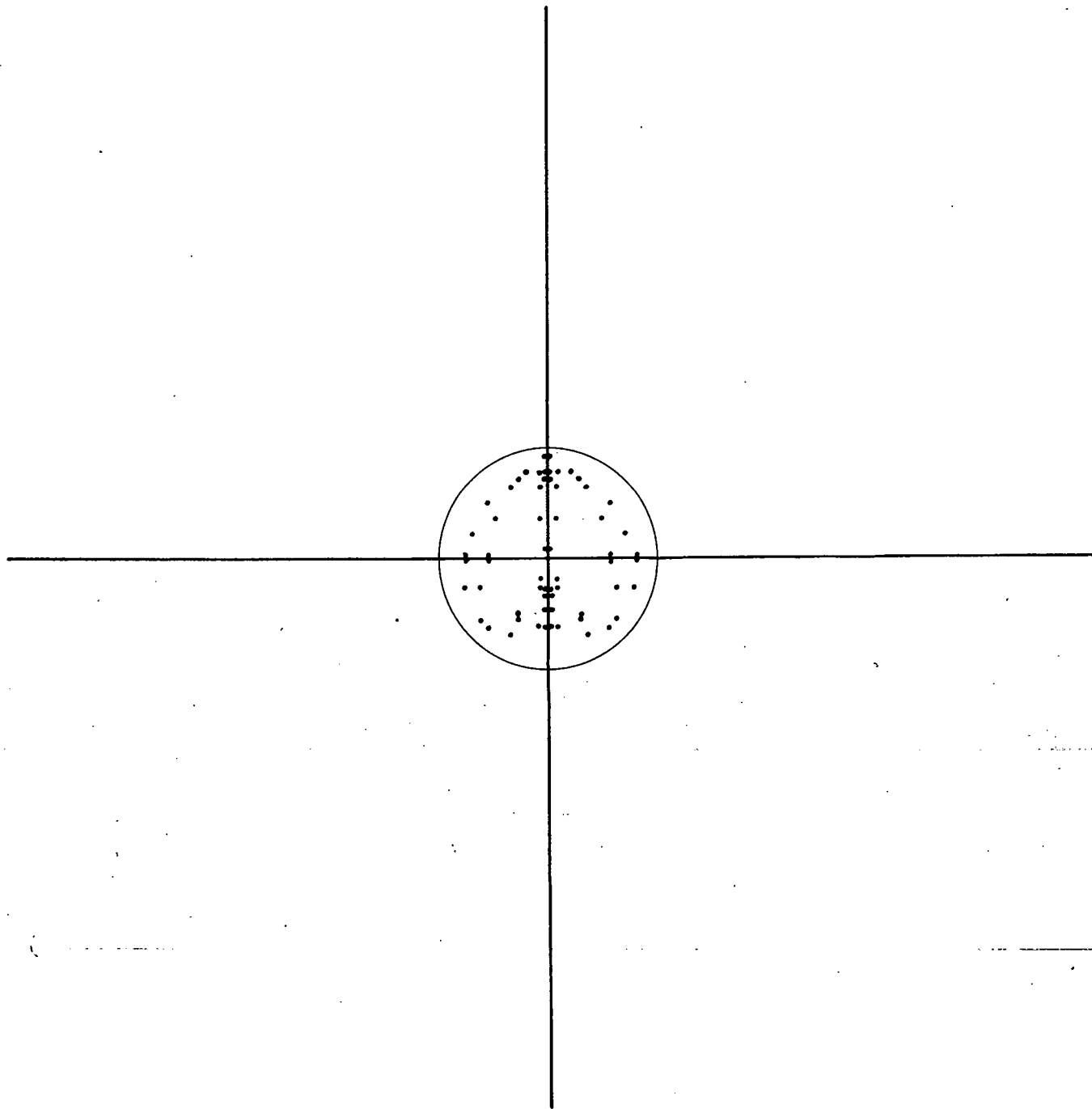


Figure 15. Spot Diagram, 4° Off-Axis $\lambda = 5893$ (D-line)

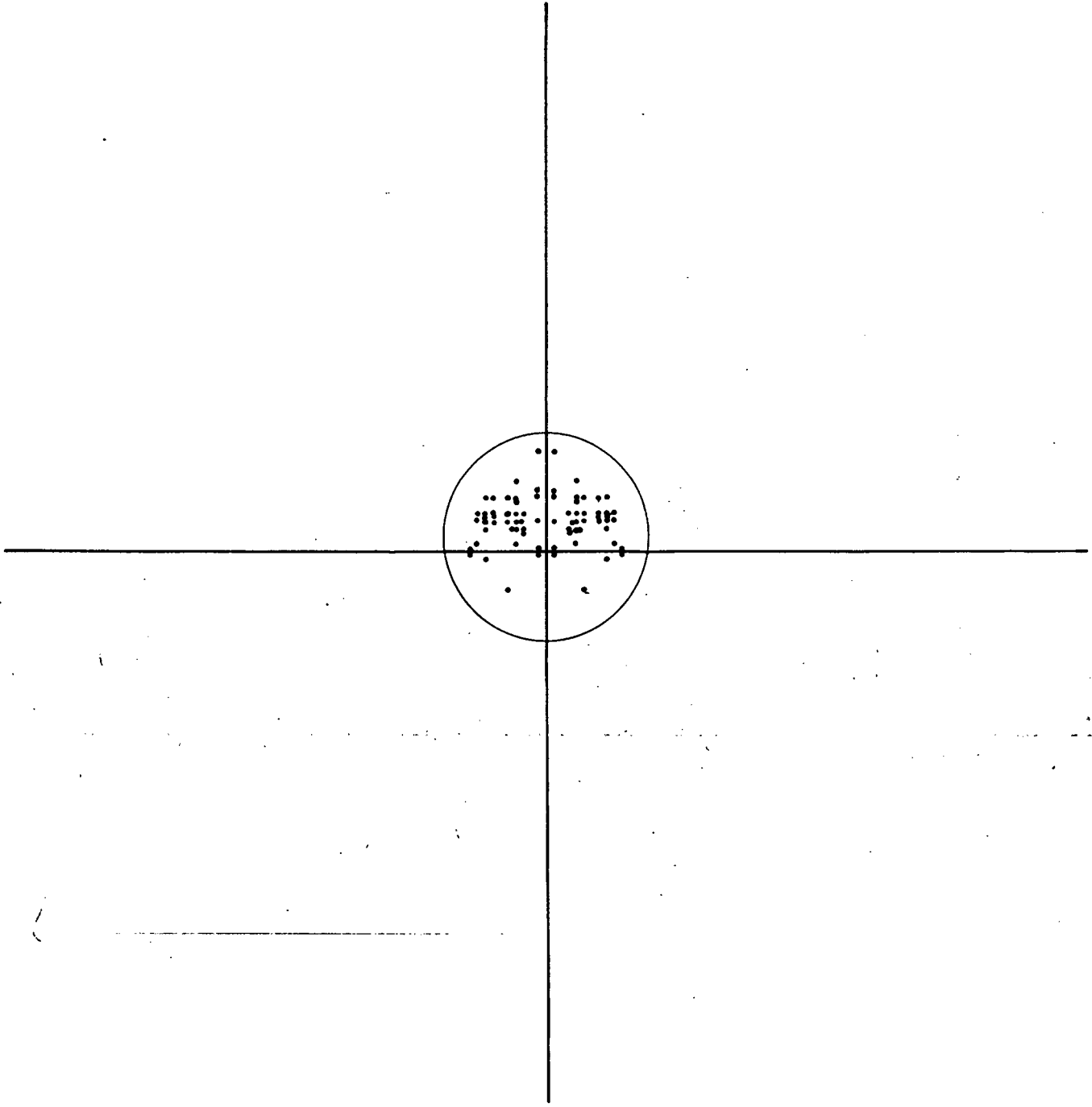


Figure 16. Spot Diagram, 4" Off-Axis $\lambda = 5461$ (e-line)

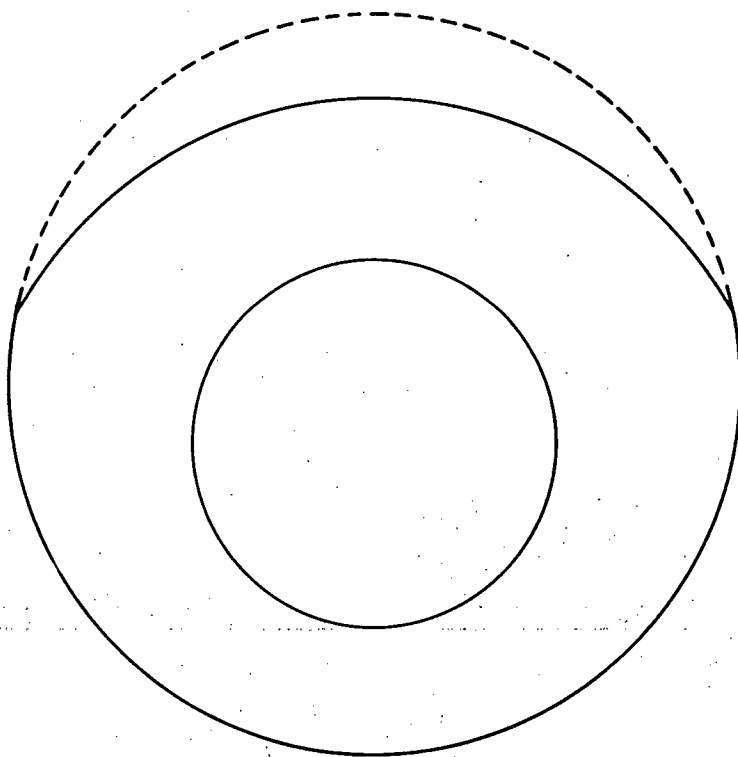


Figure 17. Pupil 5' Off-Axis

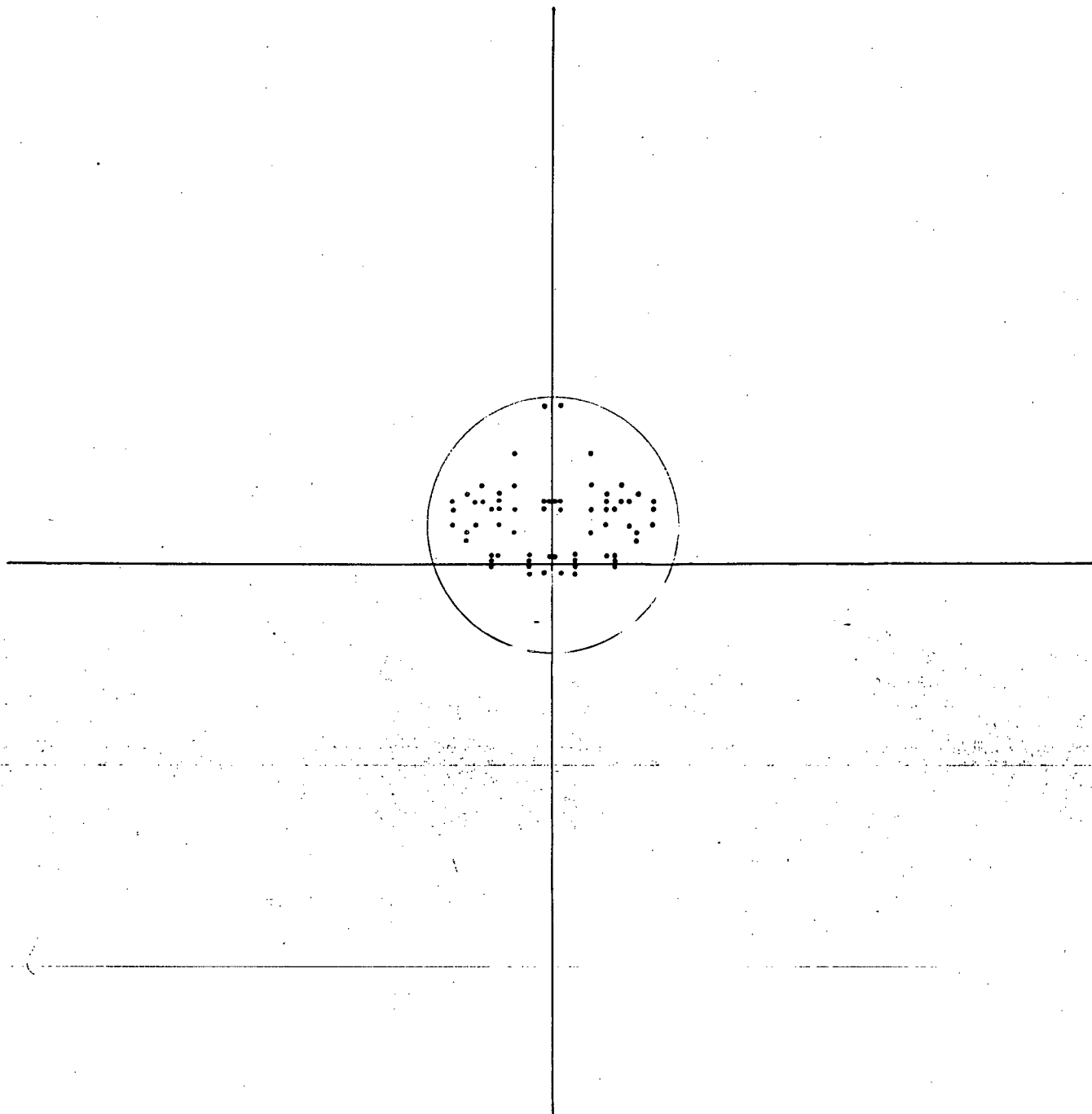


Figure 18. Spot Diagram, 5° Off-Axis $\lambda - 6563$ (C-line)

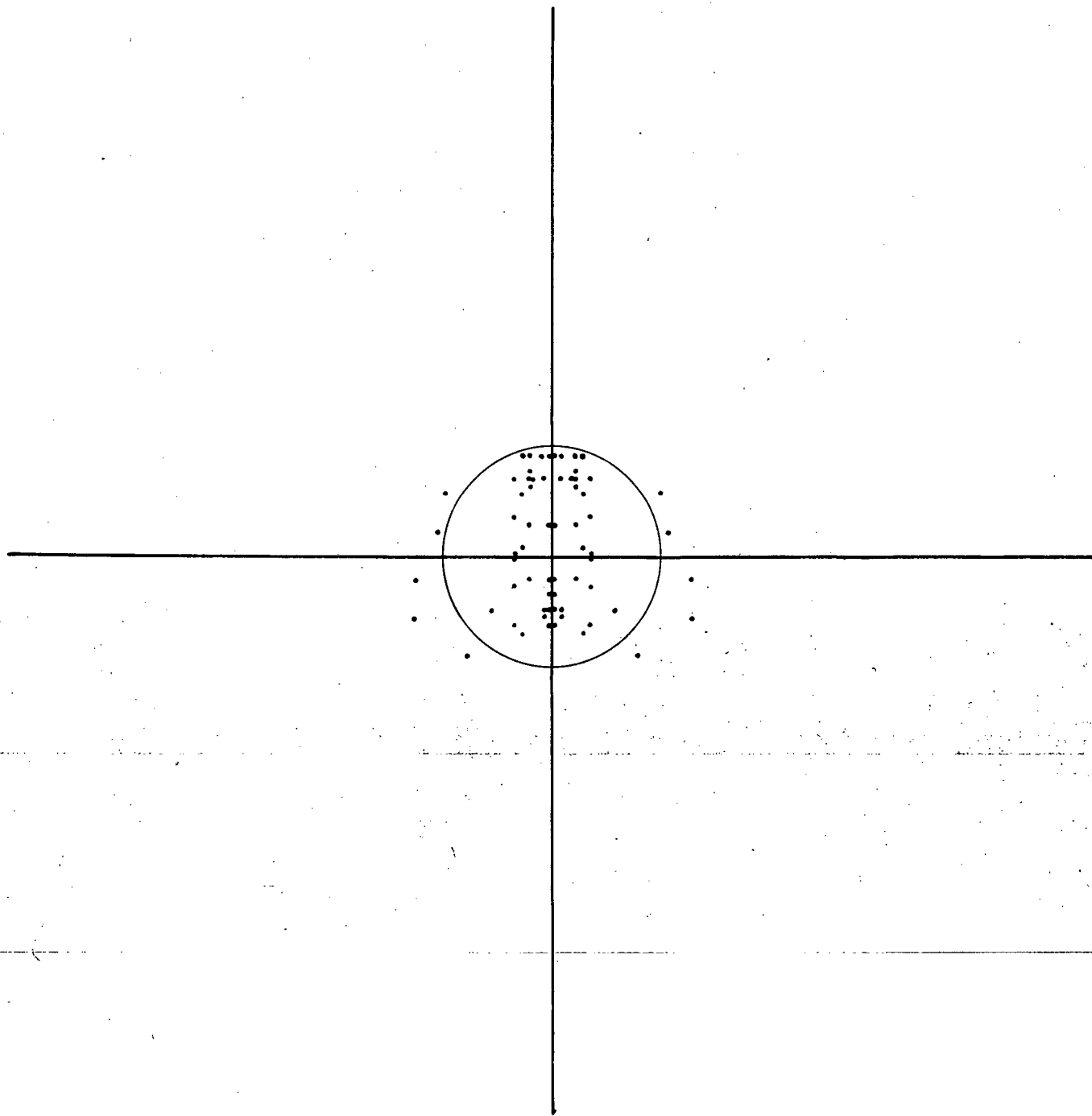


Figure 19. Spot Diagram, 5' Off-Axis $\lambda - 5893$ (D-line)

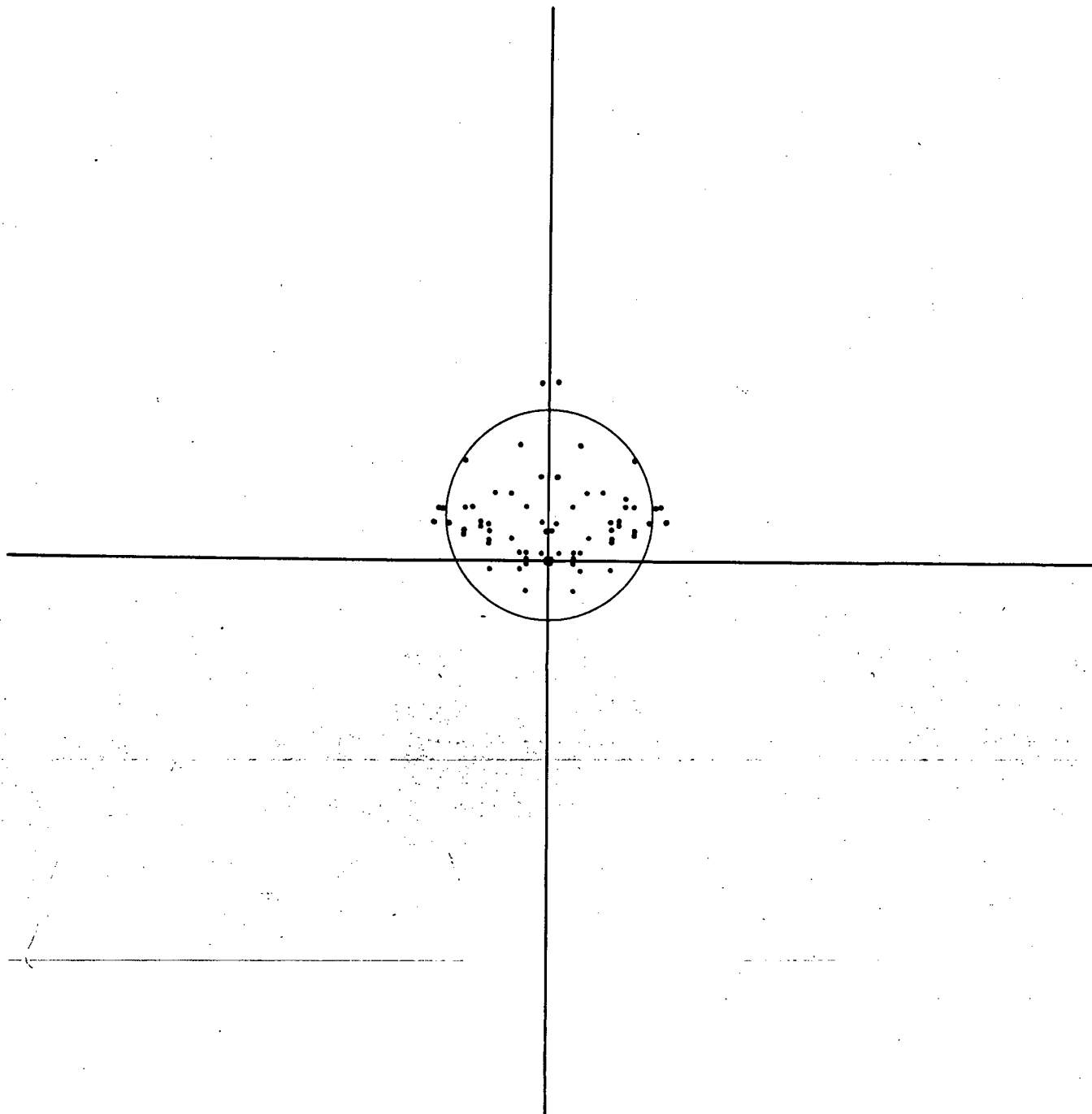


Figure 20. Spot Diagram, 5' Off-Axis $\lambda = 5461$ (e-line)

TABLE IV
CATADIOPTRIC SYSTEM
COORDINATE POINTS FOR SPOT DIAGRAMS

Axis 80 Equal Energy Points
C - LIGHT R - .00160 mm

<u>Y</u>	<u>±Z</u>	<u>Y</u>	<u>±Z</u>
+.0004	.0000	-.0004	.0000
+.0001	.0000	-.0001	.0000
-.0011	-.0000	.0011	.0000
.0004	.0001	-.0004	.0001
.0003	.0001	-.0003	.0001
-.0005	.0001	.0005	-.0001
.0003	.0003	-.0003	.0003
.0003	.0001	-.0003	.0001
-.0003	-.0001	.0003	-.0001
.0000	.0004	.0000	.0004
.0000	.0003	.0000	.0003
.0001	.0003	-.0001	.0003
-.0000	-.0000	.0000	-.0000
-.0013	-.0009	.0013	-.0009
.0000	.0001	.0000	.0001
-.0000	.0000	.0000	.0000
-.0001	-.0003	.0001	-.0003
-.0009	-.0013	.0009	-.0013
-.0000	-.0011	.0000	-.0011
-.0004	-.0015	.0004	-.0015

TABLE IV (cont'd.)			
Axis 80 Equal		Energy Points	
D - LIGHT		R = .00144 mm	
<u>Y</u>	<u>±Z</u>	<u>Y</u>	<u>±Z</u>
+.0013	+.0001	-.0013	+.0001
+.0013	.0000	-.0013	.0000
+.0001	-.0000	-.0001	-.0000
+.0010	+.0005	-.0010	+.0005
+.0013	+.0004	-.0013	+.0004
+.0008	+.0001	-.0008	+.0001
+.0008	+.0008	-.0008	+.0008
+.0010	+.0008	-.0010	+.0008
+.0008	+.0004	-.0008	+.0004
+.0001	+.0013	-.0001	+.0013
+.0005	+.0011	-.0005	+.0011
+.0008	+.0010	-.0008	+.0010
+.0008	+.0008	-.0008	+.0008
-.0000	-.0000	+.0000	-.0000
.0000	+.0013	.0000	+.0013
+.0004	+.0011	-.0004	+.0011
+.0004	+.0008	-.0004	+.0008
-.0000	-.0000	+.0000	-.0000
-.0000	+.0001	+.0000	+.0001
-.0000	-.0001	-.0000	-.0001

TABLE IV (cont'd.)			
Axis 80 Equal Energy Points			
e - LIGHT		R = .00133 mm	
<u>Y</u>	<u>±Z</u>	<u>Y</u>	<u>±Z</u>
+ .0003	.0000	- .0003	.0000
.0000	.0000	.0000	.0000
- .0013	.0000	+ .0013	- .0000
+ .0003	+ .0001	.0003	+ .0001
+ .0001	.0000	- .0001	.0000
- .0005	.0001	+ .0005	- .0001
+ .0003	+ .0003	- .0003	+ .0003
+ .0001	+ .0000	- .0001	+ .0001
- .0004	- .0003	+ .0004	- .0003
.0000	+ .0003	.0000	+ .0003
+ .0001	+ .0003	.0001	+ .0003
+ .0001	+ .0001	- .0001	+ .0001
- .0001	.0001	+ .0001	- .0001
- .0013	- .0010	+ .0013	- .0010
.0000	.0000	.0000	.0000
.0000	- .0000	+ .0000	- .0000
- .0003	- .0004	+ .0003	- .0004
- .0010	- .0013	+ .0010	- .0013
- .0000	- .0013	+ .0000	- .0013
- .0004	- .0015	+ .0004	- .0015

TABLE IV (cont'd.)			
3° 80 Equal Energy Points			
C LIGHT			
<u>ΔY</u>	<u>±Z</u>	<u>ΔY</u>	<u>±Z</u>
.0008	-.0000	.0001	-.0000
.0004	-.0000	.0000	-.0000
-.0004	-.0001	.0010	-.0000
.0008	-.0000	.0001	-.0003
+.0007	-.0001	.0000	-.0000
.0001	-.0003	.0004	-.0001
.0007	-.0001	.0001	-.0003
.0007	-.0001	.0000	-.0001
.0001	-.0005	.0003	-.0003
.0004	-.0003	.0003	-.0003
.0005	-.0001	.0001	-.0001
.0007	-.0001	.0000	-.0001
.0004	-.0004	.0000	-.0001
-.0003	-.0009	.0008	-.0007
-.0004	-.0001	.0003	-.0000
.0005	-.0003	.0001	-.0001
.0004	-.0005	.0001	-.0003
-.0001	-.0010	.0005	-.0008
.0003	-.0008	.0003	-.0005
.0001	-.0010	.0004	-.0008

TABLE IV (cont'd.)			
3° 80 Equal Energy Points			
D LIGHT			
<u>ΔY</u>	<u>±Z</u>	<u>ΔY</u>	<u>±Z</u>
+0.0014	.0000	-0.0008	.0000
+0.0013	-0.0000	-0.0013	.0001
+0.0006	-0.0000	-0.0008	.0000
+0.0013	+0.0001	-0.0007	.0001
+0.0013	+0.0001	-0.0011	.0001
+0.0009	.0000	-0.0011	.0001
+0.0008	.0004	-0.0007	.0004
+0.0011	.0003	-0.0010	.0004
+0.0009	.0000	-0.0010	.0003
.0004	.0005	.0000	.0005
.0008	.0005	-0.0004	.0007
.0010	.0005	-0.0008	.0008
.0010	.0003	-0.0010	.0008
.0005	-0.0001	-0.0008	.0003
.0004	.0009	.0000	.0009
.0006	.0008	-0.0004	.0010
.0008	.0005	-0.0006	.0009
.0005	.0000	-0.0006	.0005
.0001	.0006	.0000	.0007

TABLE IV (Cont'd.)			
4° 76 Equal Energy Points			
C LIGHT			
<u>ΔY</u>	<u>$\pm Z$</u>	<u>ΔY</u>	<u>$\pm Z$</u>
.0009	-.0001	.0005	-.0001
.0007	-.0001	.0004	-.0001
.0009	-.0004	.0013	-.0000
.0008	-.0004	.0005	-.0005
.0004	-.0004	.0003	-.0004
.0008	-.0005	.0009	-.0004
.0008	-.0005	.0004	-.0007
.0007	-.0005	.0001	-.0004
.0007	-.0007	.0005	-.0005
.0007	-.0007	.0005	-.0008
.0009	-.0007	.0004	-.0005
.0008	-.0007	.0001	-.0004
.0007	-.0004	.0001	-.0004
.0008	-.0004	.0008	-.0007
.0008	-.0007	.0004	-.0003
.0007	-.0008	.0003	-.0001
.0005	-.0003	.0001	-.0003
.0007	-.0005	.0004	-.0005
		.0003	-.0003
		.0003	-.0003

TABLE IV (cont'd.)			
4° 76 Equal Energy Points			
D LIGHT			
<u>ΔY</u>	<u>$\pm Z$</u>	<u>ΔY</u>	<u>$\pm Z$</u>
.0013	-.0000	-.0005	-.0000
.0013	-.0000	-.0009	.0000
.0013	.0000	-.0004	-.0000
.0013	-.0000	-.0004	-.0001
.0011	-.0001	-.0009	.0000
.0010	-.0000	-.0007	.0000
.0013	-.0000	-.0004	-.0000
.0013	-.0000	-.0009	.0001
.0005	.0001	-.0009	.0001
.0009	.0001	+.0001	.0000
.0011	.0001	-.0007	.0001
.0011	.0000	-.0008	.0004
.0005	.0007	-.0010	.0005
.0009	.0005	-.0008	.0004
.0010	.0004	.0000	-.0008
.0011	.0003	-.0004	.0009
.0003	.0010	-.0008	.0009
.0007	.0008	-.0009	.0008
		.0000	.0011
		-.0004	.0011

TABLE IV (cont'd.)

4° 76 Equal Energy Points

e LIGHT

<u>ΔY</u>	<u>$\pm Z$</u>	<u>ΔY</u>	<u>$\pm Z$</u>
.0004	-.0001	.0008	-.0001
.0000	-.0001	.0007	-.0001
.0005	-.0004	.0013	-.0001
.0001	-.0004	.0007	-.0005
-.0005	-.0005	.0005	-.0003
.0007	-.0007	.0009	-.0004
.0004	-.0008	.0005	-.0007
-.0001	-.0008	.0004	-.0004
.0005	-.0008	.0007	-.0004
.0007	-.0008	.0005	-.0008
.0005	-.0009	.0004	-.0007
.0001	-.0009	.0003	-.0004
.0005	-.0005	.0003	-.0003
.0005	-.0007	.0007	-.0004
.0004	-.0009	.0004	-.0004
.0000	-.0010	.0003	-.0003
.0004	-.0005	.0003	-.0003
.0003	-.0008	.0003	-.0003
		.0003	-.0004
		.0003	-.0003

TABLE IV (cont'd.)			
5° 66 Equal Energy Points			
C LIGHT			
<u>ΔY</u>	<u>±Z</u>	<u>ΔY</u>	<u>±Z</u>
.0007	-.0001	.0008	-.0001
.0008	-.0001	.0020	-.0001
.0007	-.0008	.0005	-.0007
.0007	-.0007	.0014	-.0005
.0008	-.0010	.0004	-.0011
.0008	-.0009	.0001	-.0008
.0007	-.0013	.0008	-.0007
.0008	-.0013	.0005	-.0013
.0009	-.0011	.0003	-.0011
.0010	-.0009	.0000	-.0008
.0007	-.0007	.0001	-.0007
.0009	-.0007	.0007	-.0005
.0010	-.0005	.0004	-.0005
.0005	.0001	.0000	-.0003
.0008	.0000	-.0001	-.0001
		.0000	-.0001
		.0001	.0003
		-.0001	.0003

TABLE IV (cont'd.)			
5° 66 Equal Energy Points			
D LIGHT			
<u>ΔY</u>	<u>$\pm Z$</u>	<u>ΔY</u>	<u>$\pm Z$</u>
.0010	-.0001	-.0005	-.0000
.0013	-.0000	.0004	-.0000
.0010	-.0003	-.0007	-.0001
.0011	-.0003	-.0003	-.0000
.0010	-.0005	-.0004	-.0005
.0013	-.0003	-.0009	-.0000
.0005	-.0005	-.0007	-.0000
.0008	-.0004	.0001	-.0004
.0010	-.0003	-.0003	-.0003
.0013	-.0001	-.0008	.0001
.0004	.0003	-.0010	.0004
.0009	.0003	-.0009	.0005
.0013	.0004	.0000	.0005
.0003	.0015	-.0007	.0008
.0008	.0014	-.0010	.0010
		-.0013	.0011
		-.0003	.0018
		-.0008	.0018

TABLE IV (Cont'd.)			
5° 66 Equal Energy Points			
e LIGHT			
<u>ΔY</u>	<u>$\pm Z$</u>	<u>ΔY</u>	<u>$\pm Z$</u>
.0001	-.0003	.0011	-.0001
-.0004	-.0003	.0023	-.0001
.0003	-.0008	.0009	-.0005
-.0001	-.0008	.0015	-.0004
.0004	-.0011	.0007	-.0011
.0013	-.0011	.0005	-.0008
.0005	-.0015	.0009	-.0007
.0007	-.0014	.0007	-.0014
.0005	-.0013	.0004	-.0011
.0004	-.0011	.0003	-.0008
.0005	-.0009	.0003	-.0005
.0007	-.0010	.0007	-.0003
.0005	-.0009	.0004	-.0008
.0004	-.0000	.0001	-.0004
.0005	-.0001	.0000	-.0003
		.0000	.0000
		.0001	.0001
		-.0001	.0004